X-RAY LAUE DIFFRACTION STUDY OF OXYGEN PRECIPITATES IN CZOCHRALSKI SILICON

J. Růžička, O. Caha and M. Meduňa

Department of Condensed Matter Physics, Faculty of Science, Masaryk University, Kotlářská 2, 611 37 Brno, Czech Republic
ruzmen@physics.muni.cz

Keywords:

Czochralski silicon, oxygen precipitates, x-ray Laue diffraction, statistical dynamical theory of diffraction

Abstract

In the presented article, oxygen precipitates in annealed Czochralski silicon were studied by X-ray diffraction in Laue geometry. Reflection and transmission curves obtained by measurement were compared with curves calculated using Takagi equations and statistical dynamical theory of diffraction. Parameters of the simulations were: relative volume and radii of defects the cores of which are formed by the oxygen precipitates. Spherical shapes of defects was assumed. By using these two parameters the absolute concentration of defects inside the crystal was calculated. Dependence of the parameters on pre-annealing at high temperature, on the nucleation temperature and on the duration of precipitation annealing was studied.

Introduction

When Czochralski silicon crystal is being pulled, the melt is held within a quartz crucible. The silicon melt is therefore contaminated by large amount of oxygen atoms. Most of these atoms evaporate from the melt's surface in the form of SiO oxide, but still not negligible amount of O is incorporated into the growing crystal. The concentration of this interstitial oxygen almost reaches the solubility limit in silicon [1].

Silicon wafers are submitted to series of annealing treatments during technological process in industry. Annealing at high temperature induces diffusion of oxygen atoms, which move through the crystal and gather, forming the so-called nuclei [2-3]. These nuclei can further grow and form oxygen precipitates. The precipitates contain silicon oxide SiO_x, usually SiO_2. These defects have drastic impact on electronic properties but they are also beneficial as traps for fast diffusing metal ions that can be rarely present in the crystal despite our efforts to avoid such contamination. The precipitates can also capture dislocations.

It is desirable to control the size and the concentration of the precipitates by appropriate selection of annealing parameters [3-4]. Measurement of infrared absorption spectra allows us to non-destructively determine only the concentration of interstitial oxygen before and after anneal, stochiometry and morphology of the precipitates, however the size and the concentration of the precipitates remain unknown. On the contrary etching techniques and transmission electron microscopy are destructive methods.

A non-destructive method able to determine these parameters is the X-ray diffraction, either in Bragg or in Laue geometry. In the Bragg case we usually measure maps of reciprocal space and the radius of spherical defects, whose cores are formed by the precipitates, can be determined. In the Laue case we measure transmission and reflection curves simultaneously and both the radius and the concentration of defects can be determined by comparing the measurement with the simulation. The simulation of a reflection curve can be carried out for the Bragg case as well, see for example [5] and citations therein.

Dynamical diffraction by a defect crystal

In order to study oxygen precipitates in silicon by means of X-ray diffraction the intensities of diffracted (and transmitted in the Laue case) waves coming from a disturbed crystal must be calculated. Since the precipitates are smaller than the X-ray coherence length used, ensemble averaging over all possible defect configurations must be performed. Holý and Gabrielyan [6] described the theory using statistical dynamical theory of diffraction and only key points of the calculation outline will be presented here. Only Laue case and -polarization of the primary wave will be considered for coherent and incoherent approximation in this work.

Calculation of the coherent part of the signal (i.e. we neglect the diffuse scattering) is based on Takagi equations for the case of disturbed crystals in the form

$$\hat{L}(\vec{r})\vec{d}(\vec{r}) \quad \hat{P}(\vec{r})\vec{d}(\vec{r}) \tag{1}$$

where

$$\hat{L}(\vec{r}) \quad \begin{matrix} \overline{\tilde{k}_0} & \frac{iK}{2} \; {}_hE \\ \frac{iK}{2} \; {}_hE & \overline{\tilde{k}_h} \end{matrix},$$

$$\hat{P}(\vec{r}) \quad \begin{matrix} 0 & \frac{iK}{2} \; {}_hf(\vec{r}) \\ \frac{iK}{2} \; {}_hf^*(\vec{r}) & 0 \end{matrix},$$

$$\vec{d}(\vec{r}) \quad \begin{matrix} D_0(\vec{r}) \\ D_h(\vec{r}) \end{matrix}$$

and $\tilde{k}_{0,h}$ are the coordinates in directions of real parts of the wave vectors $\vec{k}_{0,h}$, K is the magnitude of the wave vector of the primary wave, ${}_{h,-h}$ are Fourier components of the crystal susceptibility, $E \quad \langle \exp(\; i\vec{h}\vec{u}) \rangle$ is the Debye-Waller factor, $\vec{u}(\vec{r})$ is the displacement field of atoms from their

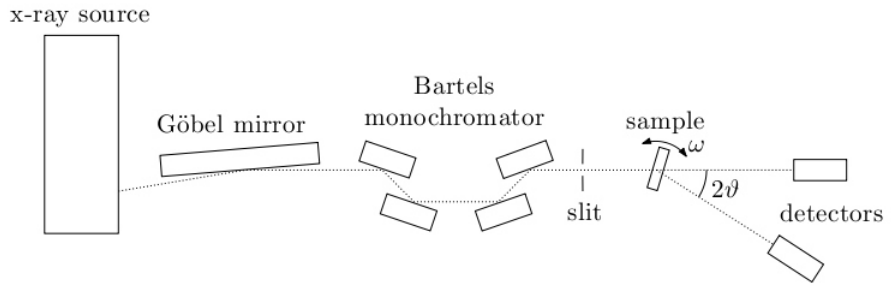

Figure 1. The layout of the HRXRD diffractometer at the Department of Condensed Matter Physics.

lattice positions, $f(\vec{r})$ exp($i\vec{h}\vec{u}$) E and $D_{0,h}(\vec{r})$ are the amplitudes of the wave fields in the crystal.

Introducing the Green's function $\hat{G}^0$ representing the inverse operator $\hat{L}^{-1}$ and performing the single-group approximation [6], Takagi equations can be rewritten into the Dyson equation in an integral form

$$\left\langle \vec{d}(\vec{r}) \right\rangle \quad \vec{d}^{\,0}(\vec{r}) \quad \int_V d\vec{r} \int_V d\vec{r}\; \hat{G}^0(\vec{r} \quad \vec{r}\,) \left\langle \hat{P}(\vec{r}\,)\hat{G}^0(\vec{r} \quad \vec{r}\,)\hat{P}(\vec{r}\,)\right\rangle \left\langle \vec{d}(\vec{r}\,)\right\rangle \tag{2}$$

where $\vec{d}^{\,0}(\vec{r})$ is the wave field in a quasiperfect crystal (i.e. a perfect crystal with susceptibility coefficients $_{h,\ h}$ $_{h,\ h}E$). Nontrivial solution can be obtained for the coherent waves in the disturbed crystal after Fourier transformation of equation (2).

Calculation of the incoherent part is performed using the ensemble averaged mutual coherence function

$$\left\langle \hat{}(\vec{r},\vec{r}\,)\right\rangle \quad \left\langle \vec{d}(\vec{r}) \quad \vec{d} \quad (\vec{r}\,)\right\rangle, \tag{3}$$

where denotes the direct product and $^+$ an adjoint vector. The solution can be obtained from Bethe-Salpeter equation in an integral form after using single-group approximation [6]

$$\left\langle \ _{ij}(\vec{r},\vec{r}\,)\right\rangle \quad {}^{c}_{ij}(\vec{r},\vec{r}\,) \int_V d\vec{r} \int_V d\vec{r}\; \left\langle G_{ik}(\vec{r} \quad \vec{r}\,)\right\rangle K_{klmn}(\vec{r} \quad \vec{r}\,)\left\langle G_{mj}(\vec{r} \quad \vec{r}\,)\right\rangle^{*}\left\langle \ _{ln}(\vec{r}\ ,\vec{r}\,)\right\rangle \tag{4}$$

where ${}^{c}_{ij}(\vec{r},\vec{r}\,)$ $\left\langle \vec{d}(\vec{r}) \quad \vec{d}(\vec{r}\,)\right\rangle$ is the mutual coherence function of the wavefield in the coherent approximation, i, j, k, l, m, $n = 0, h$, $\hat{G}(\vec{r} \quad \vec{r}\,)$ is the Green's function representing the inverse operator of the Dyson operator $\hat{D}(\vec{r})^{-1}$ $\hat{L}(\vec{r})$ $\left\langle \hat{P}(\vec{r}\,)\hat{G}^0(\vec{r} \quad \vec{r}\,)\hat{P}(\vec{r}\,)\right\rangle$ and K_{klmn} are the components of the intensity operator. Equation (4) can be solved by iterations. According to reference [6] the first iteration is sufficient and the higher ones are negligible. We consider only one incoherent scattering of each wave in the crystal; however the incoherently scattered waves can diffract again coherently.

Experiment

The experiment was performed on the high resolution X-ray diffractometer at the Department of Condensed Matter Physics at Masaryk University Brno. The layout is shown in Fig. 1. The characteristic radiation K $_1$ of molybdenum was monochromized by Göbel mirror and by Bartels monochromator (diffraction (220) by germanium single crystals). Two scintillation detectors were used in order to simultaneously measure both the transmitted and the diffracted intensities.

The samples were cut from a wafer from the top of a silicon ingot. The orientation of the ingot was (111). The thickness of the wafer was 2 mm. The samples were annealed according to the following treatment

(1150 °C/3 min) + T_n/24 h + 800 C/4 h + 1000 C/x

where the pre-annealing in the brackets was performed for some samples in order to dissolve nuclei grown during the pulling of the crystal, T_n was the nucleation temperature (500 °C or 550 °C) and x was the duration of the precipitation anneal (up to 24 hours or 48 hours respectively). The concentration of interstitial oxygen in the samples was measured by the infrared absorption spectroscopy using the IOC88 standard.

Simulation

The simulation was performed by using software written by prof. Václav Holý. The software uses the statistical dynamical theory of diffraction by a defect crystal described in reference [6]. The defects are assumed to be spherical, homogeneously distributed through the crystal and coherently nondiffracting. Simulation parameters are the radius of the defects R_{ef} and their volume V_{rel} relative to the volume of the crystal. The absolute concentration can be directly calculated using these two parameters according to the formula

$$n \quad \frac{V_{rel}}{\frac{4}{3} R_{ef}^3}, \tag{5}$$

The radii of the defects are assumed to be random values with Gaussian distribution around the given value.

It is necessary to mention that the defects are not the precipitates themselves. The surrounding silicon lattice is deformed to a great extent and this area of strong deformation does not coherently diffract as well. Therefore we in-

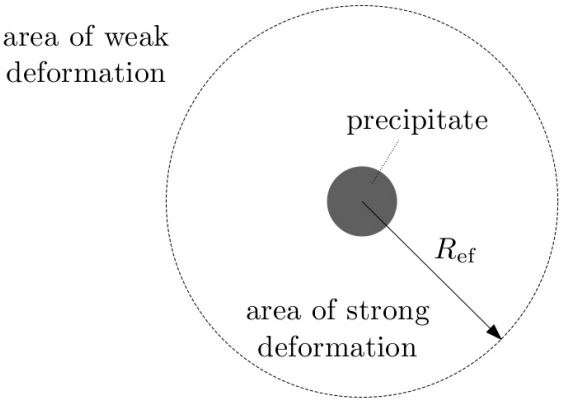

Figure 2. Schematic picture of a defect with a precipitate forming its core.

vestigate defects consisting of precipitates forming their cores and areas of strong deformation field around them. However there is also the area of weak deformation further from the precipitate which can already diffract in certain way, since the lattice is no longer deformed enough. The coherent diffraction is suppressed with respect to the one of an ideal crystal due to this fact. This weak deformation field was not considered in the performed calculation.

The described defect is schematically drawn in Fig. 2. The effective radius can be, according to Caha et al. [7], defined by the condition

$$u(R_{ef}) \quad \frac{pV}{4 \; R_{ef}^2} \quad \frac{0.1}{h}, R_{ef}^2 \quad 10\frac{pVh}{4} \qquad (6)$$

where V is the volume of the precipitate, p describes the difference between the real precipitate volume and space available in the unstrained lattice and h is the diffraction vector.

Finally the simulated curves have to be convoluted with the apparatus function consisting of the total reflection curve of the Bartels monochromator in order to be compared with the measurement. Examples of simulations and measurements are plotted for unannealed and annealed crystal in Fig. 3.

Results

The measured and simulated transmission and diffraction curves, obtained both in Laue set-up, were in good agreement only far from the coherent peak, see Fig. 3 b). We believe that the reason is neglecting the weak deformation field of the lattice which would suppress more of the coherent signal. Despite this it seems that the relative volume of the defects had been determined well. The relative volume of the defects is plotted against the duration of the precipitation anneal in Fig. 4 for all investigated samples. The error-bars in Figs. 4-8 represent the step of a simulation grid we used for finding the best fit. We can see that the precipitates grow faster with higher nucleation temperature. This effect is given by the dependence of the critical radius on temperature [1]. The growth of the precipitates in the case of pre-annealed samples is slower and the nuclei formed during the ingot growth are at least partially dissolved during the pre-annealing at 1150 C/3 min.

Opposite to the relative volume, the radii and calculated absolute concentrations of the defects were determined with large uncertainty. The radius of precipitates varied in the range from 500 nm to 800 nm for samples nucleated at 500 °C and in the range from 300 nm to 650 nm for samples nucleated at 550 °C. No significant dependency on precipitation duration was observed. The calculated precipitate concentrations are plotted in Figs. 5-6. Since the defects are the same or little smaller in size with increasing duration of the precipitation annealing, their concentration increases. This is not in agreement with the classical theory of precipitation [2] where the nuclei form only during the nucleation part of the annealing process and not during the precipitation. On the contrary the radii should increase because the longer the already formed precipitates are annealed, the bigger they grow. The problem consists in the determination of radii which is sensitive mainly to the width of the diffraction peak affected also by the coherent part. Since the model used in this paper does not include the weak de-

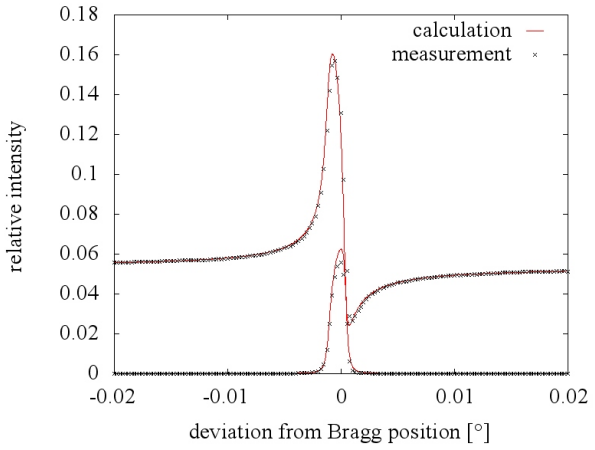

a)

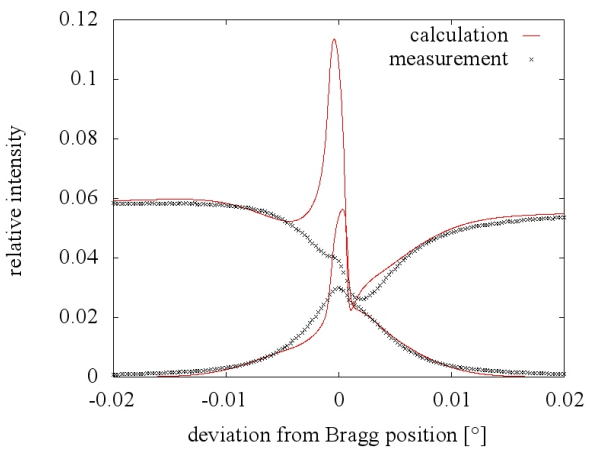

b)

Figure 3. Measured and calculated reflection and transmission curves for a) not-annealed silicon crystal (not annealed sample) and b) sample annealed at 500 °C/24 h + 800 °C/4 h + 1000 °C/48 h.

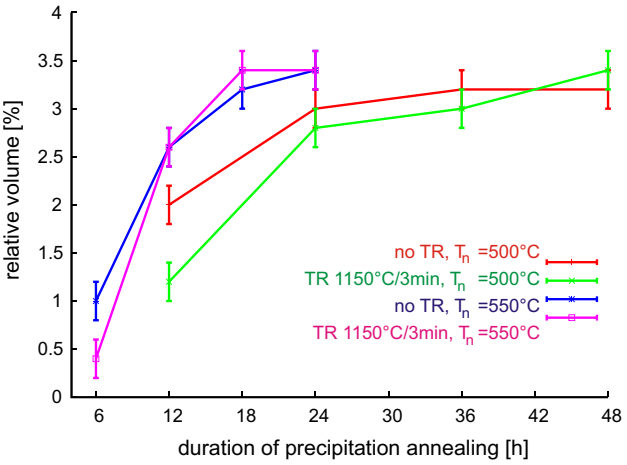

Figure 4. Determined relative volume of the defects for all studied samples.

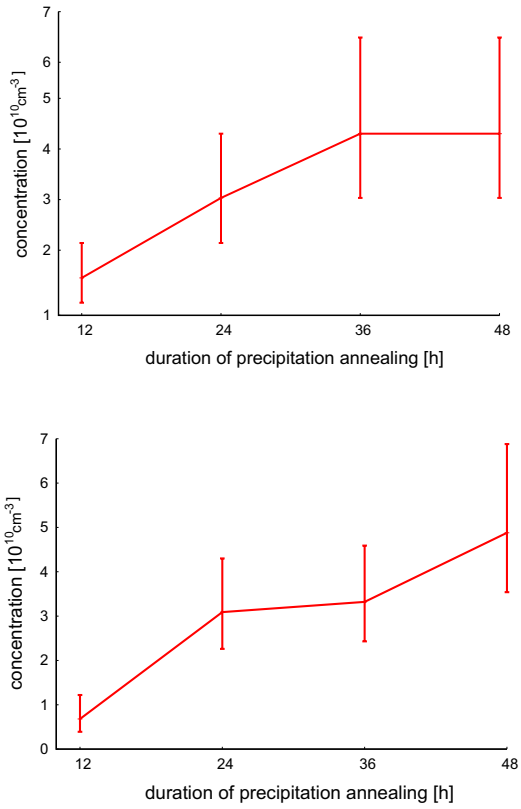

Figure 5. The absolute concentrations of defects in samples a) without and b) with the pre-anneal at 1150 C/3 h and with T_n = 500 °C.

formation field of the lattice far from the defect core, the values of the radii and consequently the values of the concentration are only approximate.

The radius of the defects is connected rather with the shape of the curves, while the relative volume is connected with the integral intensity of the reflection curve. That means that in our case, when the simulation does not fit well the measurement, it is still quite possible to get reasonable values of the relative volume since the integral intensity is more robust than the shape of the curves.

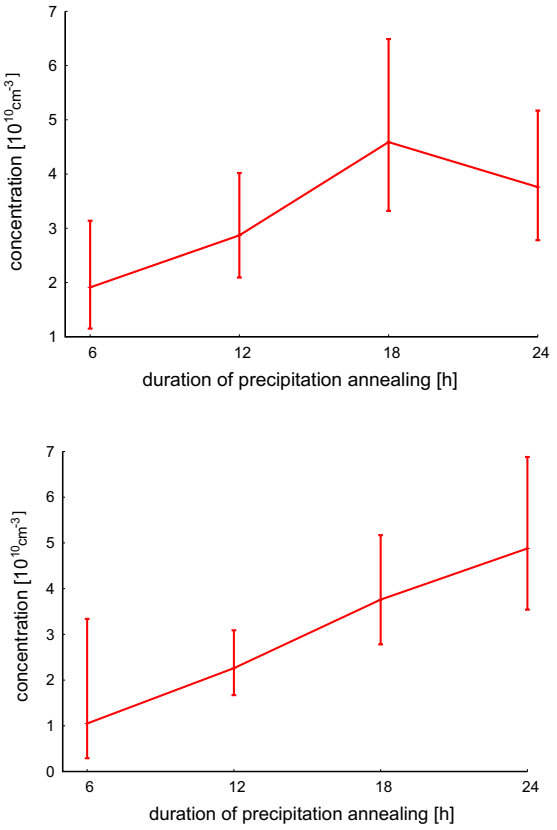

Figure 6. The absolute concentrations of defects in samples a) without and b) with the pre-annealing at 1150 °C/3 h and with T_n = 550 C.

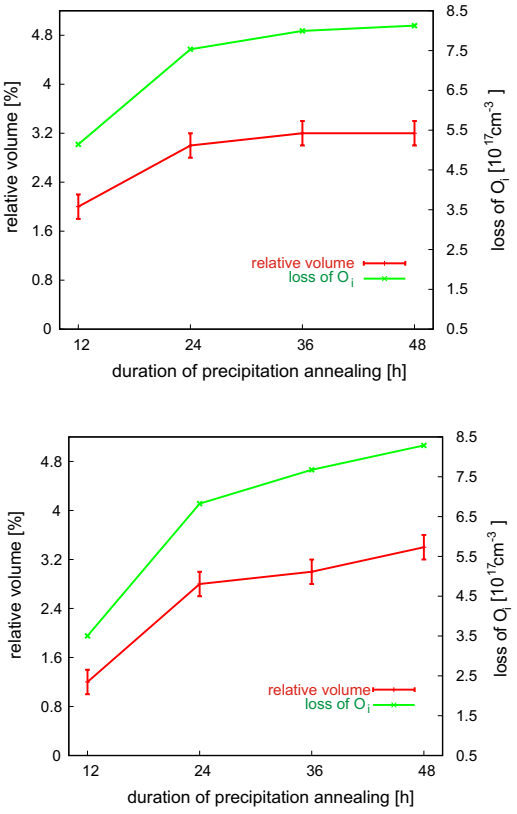

Figure 7. The relative volume of the defects compared with the loss of interstitial oxygen for samples with T_n = 500 C and a) without b) with pre-annealing.

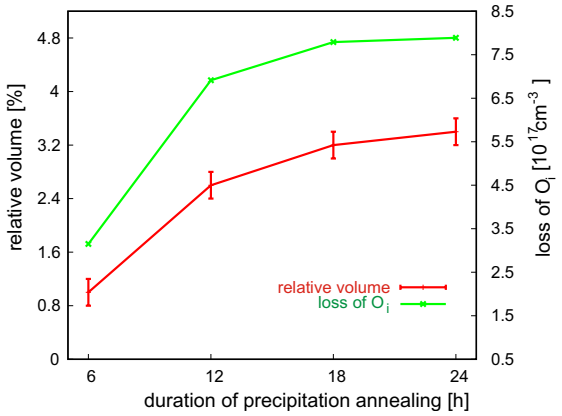

a)

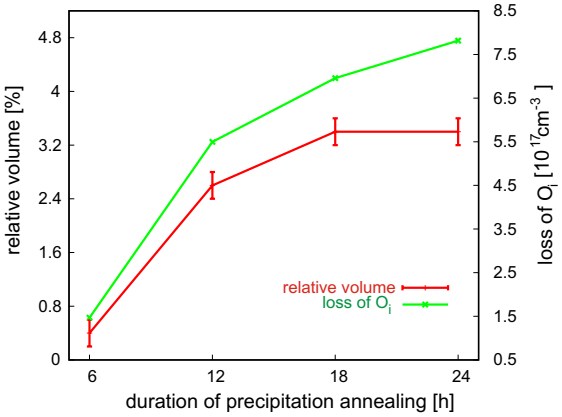

b)

Figure 8. The relative volume of the defects compared with the loss of interstitial oxygen for samples with T_n = 550 C and a) without b) with pre-annealing.

Although the relative volume is connected to the loss of interstitial oxygen, we cannot compare them quantitatively since without the information about the real size of the precipitates we cannot say how many oxygen atoms they contain. But we can compare at least the shape of the curves and it fits quite well, as seen in Figs. 7 and 8.

Conclusion

The presented method of investigating the oxygen precipitates in Czochralski silicon proved to give reasonable results of the relative volume of the defects that are in agreement with the theory of precipitation and with the infrared measurements despite the fact that the model is not completely correct. The radii of the defects and therefore consequently the absolute concentrations cannot be determined well in the current state of the model. For further investigation it is necessary to complete the model with the area of weak deformation and check whether this is truly the cause of the simulation not fitting the measurement. In case the simulated curves fit better it would be possible to combine the results of this method and of the infrared absorption measurements in order to determine the real size of the precipitates themselves.

References

1. A. Borghesi, B. Pivac, A. Sassella and A. Stella, *Journal of Applied Physics,* **77**, 1995, p. 4169.
2. K. F. Kelton, R. Falster, D. Gambaro *et al.*, *Journal of Applied Physics,* **85**, 1999, p. 8097.
3. G. Kissinger, D. Kot, J. Dabrowski *et al., ECS Transactions,* **16,** 2008, p. 97.
4. T. A. Frewen and T. Sinno, *Applied Physics Letters,* **89,** 2006, p. 191903.
5. V. B. Molodkin, M. V. Kovalchuk, A. P. Shpak *et al.*, *Dynamical Bragg and Diffuse Scattering Effects and Implications for Diffractometry in the Twenty-First Century* in *Diffuse Scattering and the Fundamental Properties of Materials*, Momentum Press, New York, 2009.
6. V. Holý and K. T. Gabrielyan, *Physica Status Solidi (b),* **140**, 1987, p. 39.
7. O. Caha, S. Bernatová, M. Meduňa, J. Buršík and M. Svoboda, submitted to Physica Status Solidi (a).

Acknowledgements

We acknowledge to prof. V. Holý for his help during discussions in theory and for providing the calculation software. This work was part of the research program MSM0021622410 of the Ministry of Education of the Czech Republic and was supported by the Czech Science Foundation project 202/09/1013.